NOTICE

CERTAIN DATA CONTAINED IN THIS DOCUMENT MAY BE DIFFICULT TO READ IN MICROFICHE PRODUCTS.

D DOE/ER/60636--3

DE91 000880

GENES AND GENE EXPRESSION: LOCALIZATION, DAMAGE AND CONTROL - A MULTILEVEL AND INTER-DISCIPLINARY STUDY

Progress Report

for period February 1, 1990 - January 31, 1991

Dr. Paul O. P. Ts'o

The Johns Hopkins University
615 North Wolfe Street
Baltimore, Maryland 21205

September 1990

Prepared for

THE U.S. DEPARTMENT OF ENERGY

AGREEMENT NO. DE-FG02-88ER60636

Introduction

A Summary of the Current Progress and Future Direction

The main objectives of this Program Project is to develop strategy and technology for the study of gene structure, organization and function in a multi-disciplinary, highly coordinated manner. The first year has been quite successful for the development of all necessary technology leading to the publication of five (5) papers.

In Project I, Molecular Cytology, the establishment of all instrumentation for the computerized microscopic imaging system (CMIS) has been completed with the software in place, including measurement of the third dimension (along the Z-axis). The technique is now at hand to measure single copy DNA in the nucleus, single copy mRNA in the cell, and finally, we are in the process of developing mathematical approaches for the analysis of the relative spatial 3-D relationship among the chromosomes and the individual genes in the interphasal nucleus. Also, we have a sensitive and reliable method for measuring single-stranded DNA breaks which will be useful for the determination of damage to DNA caused by ionizing radiation. In the coming years, we anticipate having a definitive answer concerning the three dimensional genome organization in the nucleus. Hopefully, we will use this method, together with other methods, for mapping DNA sequences along the metaphase chromosomes of humans. We also anticipate working with others, possibly with Battelle-Pacific Northwest Laboratories, to determine the radiation damage to animals caused by x-ray, radon gas and alpha particle emitters.

In Project II, the mapping of restriction fragments by 2-D enzymatic and electrophoretic analysis has been perfected for application and the results are now described in two manuscripts, either published or in press. In these papers, we describe how unknown DNA inserted in an E. coli genome can be identified and isolated without the use of a probe. Also, the arrangement of mid-repetitive DNA sequences in a mammalian genome can be individually identified. We plan to apply these powerful procedures in studying human DNA sequences by providing restriction fragment mapping/ordering of cosmids and yeast artificial chromosomes (YAC's) containing human DNA from 50-200 kilobases (kb) in size. New methods for improving resolution and sensitivities will be completed next year. We are planning to collaborate with Dr. Stylianos E. Antonarakis, at the Johns Hopkins Medical Institution, to study the genome arrangement of "line" elements in humans based on individual surveillance.

In Project III, a major finding is that the binding constant and effectiveness of antisense oligonucleotide analogues, Matagen™, can be significantly improved by substituting 2'-O-methylribos methylphosphonate backbones for the current 2'-deoxyribomethylphosphonate backbones. This improvement will increase the specificity in binding, and will significantly reduce the concentration requirement of the oligomers in experimentation. Much background studies of the triplex formation of DNA with deoxyoligonucleotides and non-ionic deoxyoligonucleoside methylphosphonates have been completed leading to the publication of two manuscripts. We are now ready to study the next step in the triplex formation - the reading of purines in a duplex by purines of the third strand as well as the structural requirement of reading purines located in two strands.

In conclusion, we expect that in the upcoming year, we will be utilizing the strategy and technology developed to answer major questions concerning the structure, organization, and functions of genes at the molecular level.

Project I

Molecular Cytology

I. **Introduction.** The approach of Project I can be summarized in three aspects.

A. Development of instrumentation and detection technology. Progress in this area includes the installation of a second Computerized Microscopic Imaging System (CMIS) and development of DNA probes for in situ hybridization containing three different types of detectors. In such a manner, three different kinds of DNA can be detected and visualized by three different chromophores in a single cell. Finally, sensitivity was enhanced so that a single copy gene can be detected and visualized. In this case, human papilloma virus #16 (HPV-16) was used as an example for demonstration.

B. Detection of DNA damage particularly that of single strand breaks at the single cell level with high sensitivity. This was achieved through the use of an antibody against cytidine which was a generous gift from Dr. Bernard Erlanger, Columbia University. Our laboratory has also developed an antibody specifically for thymidine in single strand DNA.

C. Development of approach and technology to study genome topography in the nucleus, particularly in interphase nuclei. In this case, centromeres of two chromosomes in the same nucleus were detected through specific hybridization with the use of probes for repeated DNA sequences. Thus, the stage is set for mathematical analysis of the three dimensional relative spatial relationship of these centromeres to each other using lymphocytes as a cellular model.

II. A more detailed description of our progress is outlined below.

A. New Instrumentation and Advances in DNA Probe Detection Technology

1. **Installation of a New Computerized Microscopic Imaging System (CMIS).** A second, completely new CMIS purchased with funds from the DOE University Research Instrumentation Program is now installed and operational. The new system includes:

a. A Zeiss axiovert 35 microscope complete for bright field, Normaski D/C and epi-fluorescence;

b. A Perceptic's Corporation image processing and analysis computer;

c. An Apple/Mac II image processing control computer;

d. A cooled CCD camera with 14 bit dynamic range;

e. A video Z-axis control for the microscope with rack and pinion focus control;

f. An ethernet interface for MacIntosh and VAX station II/GPX intercommunication with TSS Net Software.

Software has recently been purchased from Precision Visuals which will allow the VAX station II/GPX host computer to be utilized for image analysis, image processing, image display as well as for graphics and plotting.

2. **Preparation of DNA Probes Labelled with Different Detectors.** HPV-16 DNA was labelled with biotin or digoxigenin by nick translation or random primer extension using 5(N-[N-biotinyl-ϵ-aminocapryl]-3-aminoallyl)-2'-deoxyuridine-5'-triphosphate (Bio-ll-dUTP) or dioxigenin-ll-dUTP, respectively. The DNA was cut with a combination of Bam HI and Pst I before the primer extension reaction for reduction of the probe to an optimal size for <u>in situ</u> hybridization. A reaction time of around 2 hours or nick translation resulted in a probe size of about 200-500 base pairs (bp) as determined by gel electrophoresis.

A biotinylated DNA probe specific for the centromere of human chromosome #11 was purchased from ONCOR, Inc., and a DNA probe specific for the centromere of human chromosome #7 (ONCOR) was labelled with digoxigenin by the random primer extension reaction.

We have prepared 5(N-[2,4-dintrophenyl-ϵ-aminocaproyl]-3-aminoallyl)-2'-deoxyuridine-5'-triphosphate (DNP-11-dUTP) to enable us to label DNA with a third detector, i.e. DNP. The N-hydroxysuccinimide ester of 2,4-dinitrophenol-ϵ-amino caproic acid was prepared by reaction of N-hydroxysuccimide with DNP- aminocaproic acid in acetonitrile in the presence of dicyclohexylcarbodiimide. The product was purified by crystallization from methanol-chloroform and used to convert 5-(3-amino) allyl-dUTP to DNP-11-dUTP which was purified by elution from a DEAE-sephadex A-25 column with 0.1 to 0.9 M Et_3NHCO_3. The product, which eluted at approximately 0.6 M Et_3 $NHCO_3$, was desalted and characterized by UV-spectroscopy and NMR. DNP-11-dUTP was used to label a DNA probe specific for the centromere of human chromosome #7 in the random primer extension reaction.

3. **Localization of a Single Copy of HPV-16 DNA on Chromosome #13 of Cervical Carcinoma Cells.** <u>In situ</u> hybridization was carried out

using SiHa cells (from a cervical carcinoma) and a biotinylated HPV-16 probe or a combination of two biotinylated DNA probes, HPV-16 and one which is specific for the centromeres of both chromosomes #13 and #21. The biotinylated probes were rendered fluorescent by incubation with avidin-FITC and the signals were amplified by the use of a biotinylated rabbit anti-biotin antibody followed by a second round of avidin FITC. The chromosomes were counterstained with DAPI or propidium iodide and images were acquired with the FITC and DAPI filter combinations. Using a wide band barrier filter for FITC, one can visualize a yellow spot on each arm of an acrocentric chromosome (most likely #13) stained red with propidium iodide. Figure #2 shows the photograph of such an image after computer processing. The dual probe approach confirmed the location of the HPV on chromosome #13. Images were obtained which showed an acrocentric chromosome with a fluorescent centromere and a fluorescent spot on each of the arms. Preliminary mapping placed the virus integration site as near the junction of Q21 and Q22 on chromosome #13. In situ hybridization studies were also carried out with CaSki cells (cervical carcinoma) which contain about 500 copies of HPV. In these cells, the probe can readily be seen in the interphase nucleus as well as in a number of different chromosomes. One copy of the virus can be seen on chromosome #13 in the identical location as in SiHa cells.

B. Measurement of DNA Damage at the Single Cell Level and Cellular Response to Perturbation

1. Quantitation of DNA Strand Breaks at the Single Cell Level. DNA strand scission assay at the single cell level takes advantage of the binding of antibody to single-stranded regions of DNA. The technique is based upon the determination of the percentage of single-strandedness resulting from the time-dependent partial unwinding of cellular DNA under alkaline conditions. Single or double-stranded DNA breaks, or lesions converted to such breaks in an alkaline medium, form initiation points for unwinding. After exposure, cells were fixed immediately with cold 95% ethanol. Replicate slides of fixed cells were treated with a pH 11.9 buffer for two minutes and then neutralized. The cells were then washed with cold 70% EtOH/4% formaldehyde, cold 95% EtOH and cold 100% EtOH followed by air drying. Cells were incubated with anti cytosine antibody, washed, incubated with second antibody-FITC conjugate, washed, counterstained with DAPI and mounted in anti-fade medium. Images were obtained and processed. The fluorescence intensity per nucleus due to single-stranded DNA (FITC) normalized to DNA content (DAPI) was determined.

Figure #1 shows normalized fluorescence intensity per cell (single-stranded DNA/total DNA) plotted against dose of gamma-irradiation.

Normalized fluorescence intensity can be related to the number of DNA strand breaks, eg., 400 rads will produce about 3200 breaks per cell and yield a fluorescence intensity of about 0.77. In this experiment, we were able to detect as little as 800 breaks per cell (100 rads).

2. **Production of Differentiation - Altered Human Keratinocytes by Exposure to UV-Irradiation.** Keratinocytes were isolated from neonatal foreskins (white subjects) and cultured in serum-free low calcium (0.15 mM) medium. They were given a single dose of UV-irradiation (5.6 J/m^2, germicidal lamp) on four consecutive days and then grown in a serum-free medium containing 0.15 mM calcium for an expression time of two weeks after which the calcium concentration was increased to 0.3 mM. After one week, at 0.3 mM calcium, the concentration was increased to 0.6 mM and then, one week later, to 1.4 mM. The cells were grown for two more weeks in 1.4 mM calcium and then fixed and stained with 0.5% rhodanile blue. During this time, most cells differentiate terminally and slough from the dish leaving a few discreet foci of epidermal cells. Colonies greater than 0.5 cm in diameter were scored. Due to the high level of contamination after the lengthy culture conditions it was not possible to quantitate the results. However, large red foci (epithelial cells) appeared earlier and were more numerous in UV-irradiated plates and in positive controls (MNNG-treated) compared to non-irradiated controls.

C. Development of Approaches and Technology to Study Nuclear Topography

1. **Detection of Two Chromosome Centromeres in the Same Cell.** Human lymphocytes were stimulated to proliferate with concanavalin A and treated with colcemid before harvest. After swelling with 0.075 M KCl and fixation with MeOH:HOAc (3:1) the cells were dropped on ethanol-washed microscope slides. In situ hybridization was conducted in 2xSSC-65% formamide-10% dextran sulfate containing a biotinylated DNA probe for the centromere of chromosome #11 and a digoxigenin-labeled DNA probe for the centromere of chromosome #7. After washing, the two different probes were detected as follows:

   a. Biotin probe was rendered fluorescent by incubation with avidin-FITC and the signal was amplified by the use of a biotinylated rabbit anti-biotin antibody followed by a second round of avidin-FITC;

   b. Digoxigenin probe was rendered fluorescent by incubation with a Fab fragment of a sheep anti-digoxigenin antibody conjugated with rhodamine. The cells were then counterstained with DAPI. Images were acquired using the FITC, DAPI and rhodamine filter combinations. After computer processing, a composite

image (Figure #3) was obtained showing two red spots (chromosome #7 centromeres) and two green spots (chromosome #11 centromeres) in the same nucleus (DAPI stain). The four spots could also be observed on chromosome spreads. We now have the capability of detecting three chromosomes in one nucleus using DNP-dUTP to label the third probe which could then be detected with a blue fluorophore.

III. **Future Studies.** We will determine if genotoxic damage will lead to the synthesis of heat shock proteins, beta-interferon and/or phosphotyrosine proteins. The study will be done in a myogenic Syrian hamster cell line exposed to ionizing radiation or oxidative stress. Indirect immunofluorescence assays will be used to quantify and correlate DNA strand breaks and the above proteins at the single cell level. We will compare the ability of normal, irradiated and oxidative stressed cells to respond to normal signals for myogenic differentiation. Biotin-, DNP- and digoxigenin-labelled DNA specific for the centromeres of chromosomes #7, #11 and #17 will be prepared for use in in situ hybridization studies in unstimulated lymphocytes to determine if there is a strict and permanent association between homologous and non-homologous targets in this cellular model system. Methodology is now available to differentially label and detect the centromeres of two or three chromosomes in an interphase nucleus. Images will be acquired with our CMIS and mathematically analyzed to determine if the centromeres have a specific three dimensional spatial relationship. This same methodology will be used to conduct high resolution mapping of cosmids containing DNA fragments from chromosome #21. A human genomic library for chromosome #21 has been purchased from ATCC. Inserts will be isolated and labelled with biotin and used in in situ hybridization studies to specifically decorate this chromosome. Stacks of images at various planes through the nucleus will be obtained and processed for 3-D reconstruction studies. This will allow us to determine if interphase nuclei exhibit a cohesive territorial organization of chromosomal domains.

Publications

1. Callahan, D., Karim, A., Roby, C., Ts'o, P., Zheng, G., Lesko, S.: "Direct Visualization and Mapping of Human Papilloma Virus 16 DNA on Chromosome 13 of Cervical Carcinoma Cells," (In preparation).

2. Callahan, D., Karim, A., Roby, C., Ts'o, P., Zheng, G., Lesko, S.: "Chromosome Topography of Interphase Nuclei Studied by Double Fluorescence In Situ Hybridization and Computerized Microscopic Image Analysis," (In preparation).

3. "Mapping and Quantification of HPV-16 DNA on Chromosome 13 of Cervical Carcinoma Cells (Abstract). Submitted to Biophysical Society for the 1991 Annual Meeting.

Project II

Genome Organization and DNA Rearrangement - Investigator: Paul O.P. Ts'o, Ph.D.

I. **Introduction.** Substantial progress has been made in this project leading to the publication of two manuscripts, briefly described below and a copy listed as Appendix "A" and "B," respectively. Therefore, most of the effort was toward the development of restriction fragment order/mapping of restriction sites for a DNA fragment of approximately 50-200 kilobase (kb) in size.

A. *"A General Method for Monitoring Mammalian Genome Rearrangements Involving Sequences Neighboring Mid-Repetitive Sequences (IAP)."*

1. Utilizing mid-repetitive sequences, Intracisternal A particle (IAP) gene as a probe, genome rearrangement involving IAP genes and their neighboring sequences in rodent cells can be monitored. This is based on electrophoretic separation of the twice digested restriction fragments of genomic DNA in a 2-D pattern. The first digestion was done in solution followed by electrophoresis of the restriction fragments in the first dimension. A second restriction enzyme digestion was carried out in situ in the gel followed by electrophoresis in a second dimension perpendicular to the first electrophoresis. After Southern blotting, the DNA on the filter is hybridized with a probe which is a fragment located near the 5' end of the IAP gene, but does not overlap with the 5' long terminal repeat (LTR). The exposed x-ray film revealed about 370 distinct spots in the 2-D maps. In comparing the 2-D maps, genome rearrangement involving IAP was detected.

B. *"Enhanced Resolution of DNA Restriction Fragments - A Procedure by 2-D Electrophoresis and Double-Labelling."*

1. A probe-free method was developed to detect DNA rearrangement in bacteria based on the electrophoretic separation of twice digested restriction fragments of genomic DNA into a 2-D pattern. The first restriction enzyme digestion was done in solution, followed by electrophoresis of the restriction fragments in the first dimension. A second restriction enzyme digestion was carried out in situ in the gel, followed by electrophoresis in a second dimension perpendicular to the first electrophoresis. The 2-D pattern provides for the resolution of 300-400 spots which are defined and indexed by an "x,y" coordinate system with size markers. This approach has greatly increased the resolution power over conventional 1-D electrophoresis. To study DNA rearrangement, a 2-D pattern from a test strain was compared with the 2-D pattern from a reference strain. After the first digestion, genomic DNA fragments from the test strain were labeled with ^{35}S while those from the reference strain were labeled with ^{32}P. This was done in order to utilize the difference in the energy emission of ^{35}S and

^{32}P isotopes for autoradiography when two x-ray films were exposed simultaneously on top of the gel after the second dimension electrophoresis. The irradiation from the decay of ^{35}S only exposed the lower film, whereas the irradiation from the decay of ^{32}P exposed both the lower and upper films. By comparison, different DNA fragments existing in the test DNA and the reference DNA can be identified unambiguously by the differential two 2-D patterns produced on two films upon exposure to the ^{35}S and ^{32}P fragments in the same gel. An appropriate photographic procedure further simplified the process, allowing only the difference in DNA fragments between these two patterns to be shown in the map. We have utilized the different map obtained from E.coli HB101 and E.coli HB101 [lambda (λ)] genomic DNA to show the incorporation of one copy of λ DNA without the use of a λ DNA probe. This is the same test system which was used previously[1].

2. **Restriction Fragments ordering/mapping of restriction sites of a 100-150kb fragment.**

   a. The matrix approach developed by Fitch, et al.,[2] in ordering DNA restriction fragments obtained by a double and two single digestions, was based on a Branch and Bound technique in mathematics. This ingenious and simple approach has one problem, the uncertainty in assigning the origin of restriction fragments obtained from the double digestion in relation to the restriction fragments obtained from the single digestion. The assignment by Fitch's method is based on the accurate molecular weight measurements (in bp unit) of all fragments and the uniqueness in the relationship of the sum of all molecular weights for the doubly digested fragments to the presumptive, parental restriction fragments obtained after the single digestion (i.e., digestion by use of enzyme only). This uncertainty of assignment is totally eliminated by our current approach of two enzymes - 2-D gel treatments and display. The origins of all the doubly digested restriction fragments to the parental restriction fragments for the first/single digestion are completely and unambiguously displayed in the 2-D gel map. The only requirements are that: all the restriction fragments obtained for the first/single digestion can be completely resolved in the 1-D electrophoresis; and all the fragments must be contained and displayed within the gel. We are absolutely certain that these two conditions can be met readily, particularly with the three-

---

1 Au, L.C., Ts'o, P.O.P.: (1989) Proc. Natl. Acad. Sci. USA, 86:5507-5511.

2 Fitch, W.M., Smith, T.F., Ralph, W.W.: Gene, 22:19-29, 1983.

layers gel experiments which include DNA size marker layers. This three-layer gel experiment will provide doubly digestion fragment gel patterns twice for mutual confirmation. The conclusion will be assured further by molecular weight calculation to ensure that no small restriction fragments have been missed. The following example for solving the restriction fragments ordering obtained for EcoR2 and BamHI for λ DNA (50kb) is described.

3. Figure #4 provides the "y" coordinates for the sizes of the singly digested EcoRI fragments and the molecular sizes of doubly digested fragments. A similar figure with BamHI as the first enzyme to use, will provide the "y" coordinate for the sizes of the singly digested BamHI fragments and again the molecular sizes of the doubly digested fragments for BamHI - EcoRI treatment. From this data, the following matrix (Figure #5) is constructed: "y" coordinates show all the EcoRI fragments sizes (top to bottom, from small to large) and all the BamHI fragments sizes (again, top to bottom, small to large). The "x" coordinates show all the sizes of the doubly digested fragments (left to right, from small to large). The origin of the doubly digested fragments to the parental, singly digested fragments can be marked immediately because of the 2-D gel display. ("B" representing BamHI digested fragments, "E" representing EcoRI digested fragments, and "S" representing a once digested fragment, or fragments not digested by the second enzyme). The assignments of B's, E's, and S's all came from the 2-D gel unambiguously. A restriction map is constructed by starting with the largest fragment on the upper left column (e.g., 5505). Trace along the horizontal row until reaching the marked box S_1, then trace down along the vertical column to box E_1, followed horizontally to E_2 and again vertically upward to B_1 and so on. The tracing should alternatively be horizontal movement followed by vertical movement and vice-versa. In the meantime, when a box is reached, the order of fragment is determined according to the numerical order in the tracing. For example, the map of λ phage DNA using the combination of BamHI and EcoRI in Figure #6 is thus constructed. This 2-D gel display provides a fixed set of coordinates for each fragment obtained from the single and double digestion, thus, the various possible permutational computation for relating the doubly digested fragments to the single digested fragments as proposed by Fitch, et al., are eliminated. Our current studies indicate that with a larger gel (34cmx34cm) we should be able to separate all 30 some fragments from a 200kb human fragment in the YAC using a single restriction enzyme in the first dimension gel. Thus, this method can be applied to restriction fragments ordering/mapping for YAC's up to 200kb in size. In the case of YAC's having one megabase fragment size, this YAC will be partially digested and then electrophoresized in a pulsed-field gel electrophoresis. The partially digested fragments can be ordered

by the end labeling experiment and then these partially digested fragments can be picked up from the agarose gel for 2-D gel restriction mapping. This partial digestion-end labeling approach is outlined below. For this approach, we can provide the restriction fragment mapping for YAC's up to one to two megabase in size by the stepwise procedure in reducing these YAC's down to 200kb through partial digestion.

4. Based on the approach described above, a new simple method for linear mapping using two-enzyme digestion followed by 2-D electrophoresis has been demonstrated with λ DNA (50kb) as an example. In order to have complete coordination of DNA fragment size, all gel electrophoresis experiments were done at one time at the same condition avoiding any uncertainty. In order to demonstrate that the results on the top, middle and bottom layer gels are the same, markers are run at the edges. The results are shown in Figure #7 and Table #I. The electrophoresis patterns in 1-D and 2-D from the single and double digestions are shown in Figure #7. It should be noted that in 2-D, the same enzymes are used but the sequence is reversed, such as EcoRI/BamHI and BamHI/EcoRI. Based on these results, the constructed matrix (Figure #5) shows the relationship of all the doubly digested restriction fragments to the corresponding original single digested fragments. By tracing the matrix in the way described in application, a linear DNA restriction map for these enzymes was constructed (Figure #6).

II. **Future Direction.** Currently, we are actively in pursuit of utilizing a 2-D restriction mapping procedure to provide an order and mapping of restriction sites for the restriction fragments of human DNA sequence cloned in cosmid and yeast artificial chromosomes (YAC's). The objective is to produce a facial and reliable method which can be used for sequencing of any DNA pieces (including those containing human sequences) approximately 50-200 kb in size. In addition, we are working with Project I to align the cosmids and the YAC's along human chromosome #21 using the cytological method together with the Computer Microscopic Imaging System (CMIS). Hopefully, this tactic will provide us with a systematic approach for human genome sequencing or sequencing of other organisms. Once the general procedure is established, we can then consider the application of this method for DNA rearrangement. A possible study could be on Drosophila genome and the yeast genome.

In addition, we plan to work with the Department of Pediatrics (Stylianos E. Antonarakis, M.D.), to study the variations and rearrangements of "line" elements in human genome using the method which we have successfully employed in our paper to be published in *Analytical Biochemistry*. Using the "line" elements as probes and using the improved method of 2-D mapping, we hope to ask the question concerning polymorphism and rearrangement of "line" elements in the genome of individual humans.

Another approach is to improve the current method of resolution by the use of different electrode geometry and electrode area so as to increase the mobility of the large DNA fragments and decrease the mobility of the small DNA fragments. The results of this technology will allow us to increase resolution of large DNA fragments, while preventing the escape (loss) of small DNA fragments in the 2-D gel map. By such techniques, it is possible to increase resolutions of our 2-D gel from 2,000 fragments per gel to 3,000 fragments per gel.

The testing of this biological question is greatly assisted by the arrival of the new tools.

Project III

I.

Antisense Oligonucleotide Analogues

II. Introduction. Research in this project has made significant progress leading to the acceptance of three manuscripts for publication. The accepted manuscripts are listed as Appendix "C," "D," and "E." Progress in this area can be viewed from two areas.

A. **Organic Chemistry - Investigator: Paul S. Miller, Ph.D.** In this area, the research has indicated that a 2'-O-methylribonucleoside methylphosphonate should be considered as an alternative to the current use of a 2'-deoxyribonucleoside methylphosphonate as a backbone. This is a very significant finding and could lead to significant enhancement in the efficiency as inhibitors and thereby substantially reducing the concentration requirement of the oligomers.

B. **Physical Chemistry - Investigator: Lou Sing Kan, Ph.D.** The two papers accepted for publication describes the development of techniques in detecting triplex formation with oligonucleotides consisting of naturally occurring phosphodiester backbones, as well as the oligomers containing the 2'-deoxyribomethylphosphonates as backbones. The proton NMR spectroscopy, particularly the region of the imino-proton (NH-N) resonances occurring at very low fields, the fluorescent spectroscopy, circular dichroism spectroscopy have all been used to describe the formation of triplex formation. After the establishment of these methods for the detection of the triplex, a novel oligomer containing a 2'-O-methylribopseudo-isocytidine has been developed. The oligomer containing this analogue can form hydrogen bonds with the duplex in neutral pH for the triplex formation.

In the following sections, the abstracts of these manuscripts will be described.

A. **Organic Chemistry - Investigator: Paul S. Miller, Ph.D.**

1. Non-ionic oligo-2'-deoxyribonucleoside methylphosphonates can be used to control gene expression at the mRNA level by specifically

inhibiting translation or splicing of a selected target mRNA. Oligonucleotides and oligonucleoside methylphosphotriesters which contain 2'-O-methylribonucleosides form more stable complexes with RNA than do those which contain 2'-deoxyribonucleosides. This observation suggests that antisense oligonucleoside methylphosphonates in which 2'-O-methylribonucleosides replace 2'-deoxyribonucleosides should show enhanced stability when interacting with their target nucleic acids. r-$U^mpI^mA^mU^mC$ was prepared, where N^m represents a 2'-O-methylribonucleoside and the underline shows the position of the methylphosphonate linkages. r-$U^mpI^mA^mU^mC$ forms a stable duplex with r-GAUCA (T_m 21°C in 0.1 M NaCl, 50 mM Tris) whereas the corresponding duplex formed by an oligo-2'-deoxyribonucleoside, d-TpGATC/r-GAUCA, melted at a significantly lower temperature (T_m 18°C). These results suggest that oligo-2'-O-methylribonucleoside methylphosphonates should show enhanced efficacy as inhibitors of gene expression at the mRNA level.

Report. The expression of normal or altered genes can be studied using antisense oligonucleotides[3]. Non-ionic oligo-2'-deoxyribonucleoside methylphosphonates have been used to control gene expression at the mRNA level by specifically inhibiting translation or splicing of a selected target mRNA[3,4,5,6]. These oligomers, forming stable duplexes with single-stranded DNA and RNA, are resistant to nuclease hydrolysis and are readily taken up intact by mammalian cells in culture. The oligomers inhibit mRNA translation of mRNA splicing 50%-90% in the concentration range of 100 - 150 μM. The inhibitory efficacy of the methylphosphonate oligomers can be improved by appending cross-linking groups such as psoralen to the oligomers[7,8,9,10].

---

3 Cohen, J.C. (ed) 1989. Oligodeoxyribonucleotides. Antisense Inhibitors of Gene Expression. Topics in Molecular and Structural Biology 12. MacMillan Press London.

4 Miller, P.S. and Ts'o,P.O.P. 1988. Oligonucleotide Inhibitors of Gene Expression in Living Cells: New Opportunities in Drug Design. Annual Reports Med. Chem. 23, 295-304.

5 Miller, P.S. 1990. Antisense nucleic acid analogues as potential antiviral agents. in Herpesviruses, the Immune System and AIDS. L. Aurelian ed. pp 343-360 Kluwer Academic Publishers Boston.

6 Miller, P.S. 1990. Antisense oligonucleoside methylphosphonates. in Antisense RNA and DNA, J.A.H. Murray ed. J. Wiley and Sons, New York in press.

7 Lee, B.L., Murakami, A., Blake, K.R., Lin, S.-B. and Miller, P.S. (1988) *Biochemistry 27*, 3197-3203.

8 Kean, J.M., Murakami, A., Blake, K.R., Cushman, C.D. and Miller, P.S. (1988) *Biochemistry 27*, 9113-9121.

9 Lee, B.L., Blake, K.R. and Miller, P.S. (1988) *Nucleic Acids Res. 16*, 10681-10697.

Upon photo-activation, these derivatized oligomers form covalent complexes with targeted mRNA and inhibit translation 50% - 70% at oligomer concentrations of 5 μM[8].

Another method of increasing the inhibitory efficacy is design methylphosphonate oligomers which form inherently more stable duplexes with mRNA. Previous studies have shown that oligonucleoside ethylphosphotriesters which contain 2'-O-methylribonucleosides form more stable complexes with transfer RNA than do those which contain 2'-deoxyribonucleosides[11]. Similarly, oligo-2'-O-methylribonucleotides form duplexes with complementary oligoribonucleotides which have higher melting temperatures (Tms) than duplexes formed by oligo-2'-deoxyribonucleotides of the same sequence[12]. These observations suggested that antisense oligonucleoside methylphosphonates in which 2'-O-methylribonucleosides replaced 2'-deoxyribonucleosides might show enhanced stability when interacting with their target nucleic acids.

To test this possibility, we prepared r-U^mp$\underline{I^m A^m U^m C}$, where N^m represents a 2'-O-methylribonucleoside and the underline shows the position of the methylphosphonate linkages[13]. The internucleotide linkage at the 5'-terminus of the oligomer is a phosphodiester group. The required 2'-O-methylnucleosides were prepared by literature procedures[14,15]. These were converted to 5'-O-dimethoxytrityl-3'-O-methyl-N,N-diisopropylaminophosphonamidites by reaction of the 5'-O-dimethoxytrityl-2'-O-methylribonucleoside with methyl dichlorophosphite followed by reaction with diisopropylamine in the presence of ethyldiisopropylamine. The overall yield starting from the 2'-O-methylribonucleoside was 60% to 65%. The 6-amino group of A^m was protected with a phenoxyacetyl group.

The phosphonamidite synthons were used to prepare r-U^mp$\underline{I^m A^m U^m C}$ on a Biosearch Model 8700 DNA synthesizer. Controlled pore glass

---

[10](...continued)

[10] Bhan, P. and Miller, P.S. (1990) *Bioconjugate Chemistry 1*, 82-88.

[11] Miller, P.S., Braiterman, L.T. & Ts'o, P.O.P. (1977) *Biochemistry 16*, 1988-1996.

[12] Inoue, H., Hayase, Y., Imura, A., Iwai, S., Miura, K. & Ohtsuka, E. (1987) *Nucleic Acids Res. 15*, 6131-6148.

[13] Miller, P.S., Bhan, P., Cushman, C.D., Kean, J.M. and Levis, J.T. (1990) *Nucleosides and Nucleotides* 9, in press.

[14] Sproat, B.S., Beijer, B. & Iribarren, A. (1990) *Nucleic Acids Res. 18*, 41-49.

[15] Yano, J., Kan, L.S. & Ts'o, P.O.P. (1980) *Biochim. Biophys. Acta 629*, 178-183.

derivatized with N-benzoyl-5'-dimethoxytrityl-3'-O-*t*-butyldimethylsilylcytidine was used as the support. The phosphonamidite synthons were used at a concentration of 0.065 M and the coupling time was 15 minutes for each synthetic cycle. The last (5'-) nucleotide unit was added as the 5'-O-dimethoxytrityl-2'-O-methyluridine-3'-O-N,N-diisopropylamino-β-cyanoethyl phosphoramidite. The average coupling yield was 96%, which is comparable to the average coupling yields obtained in syntheses of oligo-2'-deoxyribonucleoside methylphosphonates.

The oligomer was deprotected and simultaneously removed from the support by sequential treatment with hydrazine hydrate in pyridine-acetic acid buffer followed by treatment with ethylenediamine in 95% ethanol (1:1 v/v). The oligomer with the 2'-O-*t*-butyldimethylsilyl group still attached, was purified by DEAE cellulose chromatography followed by reversed phase HPLC and was obtained in 46% overall yield. The silyl protecting group was removed quantitatively by treating the oligomer with 0.05 N HCl in acetonitrile/water (2:1) at 37°C for 20 hours.

The stability of the duplex formed between r-$U^mpI^mA^mU^mC$ and an oligo-RNA target, r-GAUCA, was compared with those of similar duplexes formed by d-TGATC and with d-TpGATC in 50 mM Tris or 50 mM Tris containing 0.1 M NaCl at a total oligomer strand concentration of 20 μM. The melting temperatures of the various duplexes are shown in Table II. r-$U^mpI^mA^mU^mC$ forms a stable duplex with r-GAUCA whose melting temperature of the duplex with increasing ionic strength. This effect most likely results form the reduced charge repulsion between the 5'-phosphodiester linkage of r-$U^mpI^mA^mU^mC$ and the negatively charged backbone of the target. A rather broad transition curve is observed which is reflective of the short length of the oligomer.

The d-TpGATC/ r-GAUCA duplex melted over a broader range than did r-$U^mpI^mA^mU^mC$ /r-GAUCA and had a significantly lower melting temperature in 50 mM Tris. The melting temperature of r-$U^mpI^mA^mU^mC$/r-GAUCA was similar to that of d-TGATC/r-GAUCA under both salt conditions, although the transition curves of the r-$U^mpI^mA^mU^mC$-duplex were somewhat sharper. The I^m residue of r-$U^mpI^mA^mU^mC$ forms only two hydrogen bonds with C whereas the G residues of d-TGATC and d-TpGATC each form three hydrogen bonds. Thus one would expect a further increase in the stability of the oligo-2'-O-methylribonucleoside methylphosphonate if the more difficult to synthesize G^m is substituted for I^m.

B. **Physical Chemistry - Investigator: Lou Sing Kan, Ph.D.**

1. *"Proton NMR and Optical Spectroscopic Studies on the DNA Triplex Formed by d-A-(G-A)7-G and d-C-(T-C)7-T."* Triplex and duplex formation of two deoxyribohexadecamers d-A-(G-A)7-G (a) and d-C-(T-C)7-T (b) have been studied by UV, CD, fluorescence, and proton NMR spectroscopy. Optical studies of (a) and (b) at dilute concentrations (μM range) yielded results similar to those seen for polymers of the same sequence, indicating that these hexadecamers have properties similar to the polymers in regard to triplex formation. The CD spectra of concentrated NMR samples (nM range) are similar to those observed at optical concentrations at both low and high pH, making possible a correlation between CD and NMR studies. In NMR spectra, two imido NH-N hydrogen bonded resonance envelopes at 12.6 and 13.7 ppm indicate that only the duplex conformation is present at pH > 7.7. Four new NH-N hydrogen-bonded resonance envelopes at 12.7, 13.5, 14.2 and 14.9 ppm are observed under acidic conditions (pH 5.6) and the two original NH-N resonances gradually disappear as the pH is lowered. Assignment of these four peaks to Watson-Crick G-C, Hoogsteen T-A, Watson-Crick A-T, and Hoogsteen C+-G hydrogen-bonded imidos, respectively, confirm the formation of triple-stranded DNA. There may be a dangling C+ base on the third strand in the triplex (From intensities of these signals) indicating that the homopyrimidine third strand has the same polarity as the homopurine strand. These studies also show that triplex is more stable than duplex at the same salt condition and that triplex melts to single strands directly without going through a duplex intermediate. However, in the melting studies, a structural change within the triple-stranded complex is evident at temperatures significantly below the major helix-to-coil transition. These studies demonstrate the feasibility of using NMR spectroscopy and oligonucleotide model compounds (A) and (b) for the study of DNA triplex formation.

2. *"Comparative Circular Dichroism and Fluorescence Studies of Oligodeoxyribonucleotide and Oligodeoxyribonucleoside Methylphosphonate Pyrimidine Strands in Duplex and Triplex Formation."* An analogue of the homopyrimidine oligodeoxyribonucleotide $d(CT)_8$ has been synthesized. This analogue $d(\underline{CT})_8$ contains non-ionic methylphosphonate internucleoside linkages. The pH-dependent conformational transitions of $d(\underline{CT})_8$ have been studied and its ability to form duplexes and triplexes with the normal homopurine oligonucleotide $d(AG)_8$ has also been investigated as a function of pH. Circular dichroism spectroscopy and ethidium bromide fluorescence enhancement have been used to monitor pH-dependent conformational transitions driven by the protonation of cytosine residues, and the different behavior of $d(\underline{CT})_8$ and $d(CT)_8$ has been compared. It was possible to form self-associated complexes using either $d(CT)_8$ or $d(\underline{CT})_8$ and both compounds combined with $d(AG)_8$ to form duplex or triplex DNA. Self-associated complexes of $d(\underline{CT})_8$ had a greater degree

of structure than self-associated complexes of $d(CT)_8$ and in both cases complexes formed at an apparent pK, of 5.5. At neutral pH, the CD spectrum of $d(AG)_8 \cdot d(\underline{CT})_8$ duplex was quite different from the CD spectrum of $d(AG)_8 \cdot d(CT)_8$ duplex, reflecting most likely a difference in conformation. The duplex to triplex transition characteristic of this DNA sequence occurred at a lower pH when $d(\underline{CT})_8$ was substituted for $d(CT)_8$; however, at pH 4.2 triplex containing $d(\underline{CT})_8$ was similar in conformation to triplex containing $d(CT)_8$. Several of these observations can be related to the alterations in electrostatic and steric interactions that occur when the negatively charged phosphodiester backbone of $d(CT)_8$ is replaced with a non-ionic methylphosphonate backbone.

3. *"Triplex Formation of Oligonucleotides Containing 2'-O-Methylpseudo-isocytidine in Substitution of 2'-Deoxycytidine."* The formation of triple-stranded nucleic acid helices (triplex) has been studied in systems consisting of RNA and/or DNA strands. In recent years, studies of sequence specific triplex formation of short synthetic oligonucleotides (or their analogues) are of prime interest. A triplex can be formed as a triad consisting of a homopyrimidine strand, a homopurine strand and a homopyrimidine strand. The third strand (i.e., the second pyrimidine strand) is located in the major groove of a duplex with Watson-Crick base pairing. Thymines or cytosines in the third strand form Hoogsteen type hydrogen bondings with adenines and guanines in the homopurine strand respectively. Since protonation of cytosine bases in acidic conditions is essential in order to provide the second hydrogen bonding between the protonated cytosine and guanine in the Hoogsteen pair of the triad (Figure #8a), this C-G-C+ triad is unstable in physiological conditions. This requirement limits the formation of triplex in living cells since the cellar pH is usually above pH 7.0. To overcome this limitation, we designed and synthesized an oligonucleotide containing 2'-O-methylpseudo-isocytidine, *1* (Figure #8) which may form Hoogsteen type base pairing through hydrogen bondings with guanine in neutral and basic conditions (Figure #8b). As indicated in the figure, this nucleoside *1* already contains one hydrogen at the N-3 position for hydrogen bonding with the guanine in the Hoogsteen pair of the triad. A scheme for the synthesis of *1* and its amidite synthon *9* is shown in Figure #8c. An octamer 5'(TT*1* TT*1* TT)3', a was synthesized on a DNA synthesizer and purified by C-18 HPLC.

We studied a triplex formation of the oligomer a with an undecameric target duplex 5'd(AAGAAGAAGAA)3' - 5'd(TTCTTCTTCTT)3', d. Both 5'd(TTCTTCTT)3', b and 5'(TTCmTTCmTT)3', c (Cm = 2'-O-methylcytidine) were used as controls for third strand. An octamer a or b or c was mixed with the duplex d in a buffer, and the thermally induced transition of the helices in each mixture was studied by measuring the UV absorption at 260 nm at pH 7.0 (Figure #9a). Both

the duplex d alone and the mixtures consisting of b and d, or c and d showed only one transition (Tm = 42° C, Figure #9b) which was attributable to the melting of the duplex d itself. On the other, the mixture of a and d showed two transitions (Figure #9b). One transition (Tm = 42° C) was identical with the melting of d and the second transition (Tm = 12° C) was surmised to be the dissociation of the third strand a from the duplex d as illustrated in Figure #9a. This mixture of a and d showed similar transition profiles between pH 7.0 and pH 8.7.

Also, we studied the circular dichroism (CD) spectra of mixtures of oligomers. Spectra of the mixture of a and the duplex d at both 3° C and 30° C in neutral condition are shown in Figure #10a and Figure #10b. A controls, the CD spectra of the mixture of undecamers, 5'd(AAGAAGAAGAA)3' and 5'd(TTC1TCTTCTT)3' in 1:2 molar ratio respectively, at both pH 5.5 and pH 7.0 at 3° C are shown in Figure #10c and Figure #10d). The control mixture showed a large negative band at 215 nm (Figure #10c) in the acidic condition in which the oligomers were in triplex form. On the other hand, the negative band 215nm was undetectable in the neutral condition in which the triplex dissociated into a duplex and single strand (Figure #10d). This negative CD bad is considered as an indication. At 3° C, similar to the control triplex at acidic pH, the mixture of a and d showed a negative band at 215nm (Figure #10a), indicating the formation of the a - d triplex. In contrast, at 30° C, the spectrum of the mixture of a and d was similar to that of the control mixture of a duplex and a single strand at neutral pH (Figure #10b). This change in the CD spectra was not caused by any conformational alteration of the duplex d itself or the octamer a itself because between 3° C and 30°, the individual CD spectra of d and a were not notably different. Therefore, the CD spectrum i Figure #10a indicated the formation of the a - d triplex. However, the complex of a - d is not a complete triplex but is a chimera of a triplex part and a duplex part as shown in Figure #9, because of the disparity in length of *a versus* d. Therefore the CD spectrum in Figure #10a was inferred to be the sum of the spectral contributions from the triplex part and from the duplex part, and the magnitude of the negative band at 215 nm in Figure #10a was expected to be smaller than that of the spectrum of control triplex (Figure #10c).

In a recent report, the substitution of 2'-deoxycytidine by 2'-deoxy-5-methylcytidine ()^{m}C) and the substitution of thymidine by 2'-deoxy-5-bromouridine in an oligomer can cause the formation of triplex above neutral pH. Under such a situation, the substitution, at position #5 of pyrimidines was able to add a stabilizing factor for the triplex. Our approach is very different. By designing an oligonucleotide containing a 2'-deoxycytidine analogue which contains a hydrogen at N-3 (or N-

1) position and which can form a pair of hydrogen bonding with 2'-deoxyguanosine in the Hoogsteen scheme through this very hydrogen, a triplex can be formed without the requirement of protonation. With this innovative approach, it is anticipated that the possibility of triplex formation of an oligonucleotide analogue with genomic DNA in mammalian cells can be tested.

Figure Legends

Figure #1. The relationship between the amount of single-stranded DNA (FITC fluorescence) per cell, normalized to total DNA content (DAPI fluorescence) and dose of gamma irradiation administered to cells. The number of DNA strand breaks per cell is related to fluorescence intensity, i.e., single-stranded DNA, as follows: 3,200 breaks per cell yields a normalized fluorescence intensity of approximately 0.77.

Figure #2. A Computer-generated composite image of chromosomes from SiHa cells shown in false color. A single copy of the HPV-16 virus, stained with FITC can be seen on each arm of chromosome #13 which is directly over the two micron bar. The chromosomes were counterstained with propidium iodine. Virus was detected by in situ hybridization with a biotin-labelled DNA probe.

Figure #3. Computer-generated composite image of a human lymphocyte nucleus shown in false color. The centromeres of the two chromosomes #11 homologues, stained with FITC, and the centromeres of the two chromosomes #7 homologues, stained with rhodamine, can be seen in the nucleus which is counterstained with DAPI. The centromeres for chromosome #11 and chromosome #7 were detected by in situ hybridization with a biotin- and a digoxigenin-labelled probe, respectively.

Figure #1

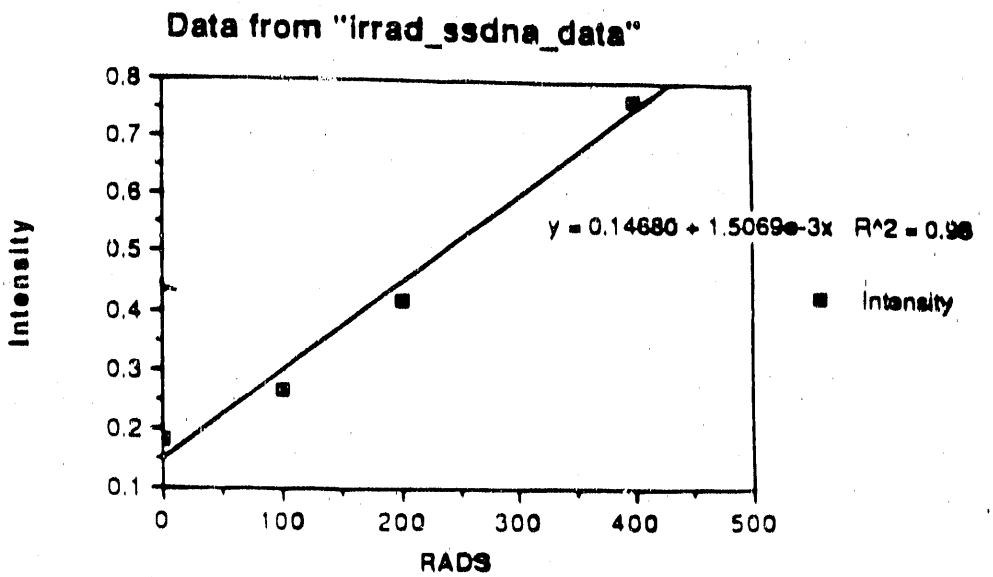

X-ray

~2 x 10^{-12} breaks/rad/dalton DNA

Diploid hamster cells contain ~4 x 10^{12} daltons of DNA

100 rads = 800 breaks/cell

400 rads = 3200 breaks/cell

2 MICRONS
STAGE III
INFECTED

centro.
11.7

Figure #4

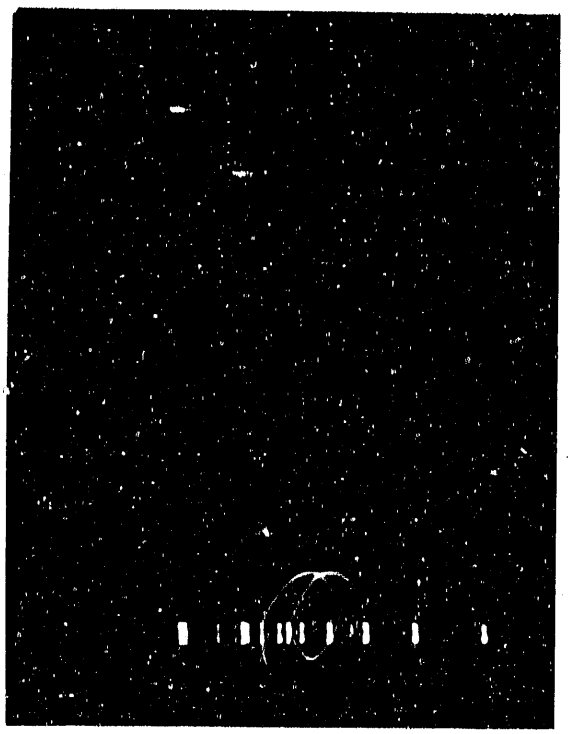

2-D pattern of DNA restriction fragments (lambda Hind III) and DNA size markers (1 kb DNA ladder) in the middle gel of three-layer electrophoresis.

Figure #5

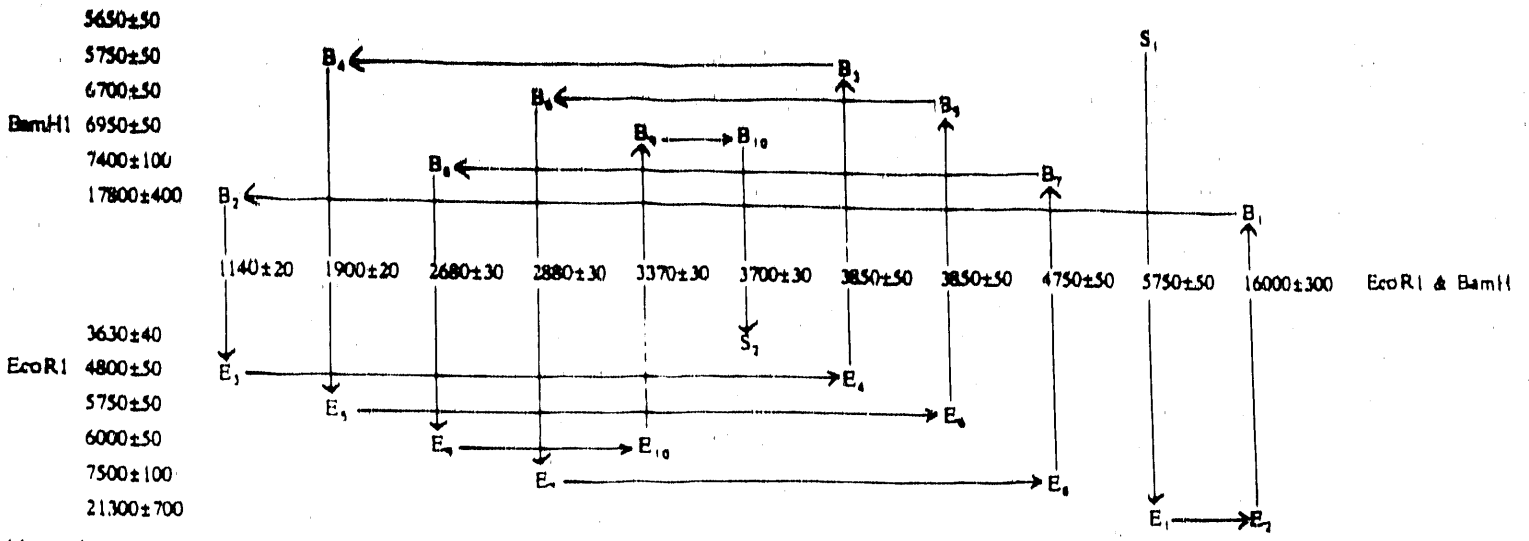

Matrix for construction of the linear restriction fragment map of λ phage DNA. The left-most vertical column shows all the BamH1 digested fragment sizes in the upper half and all the EcoR1 digested fragment sizes in the lower half (top to bottom, small to large). The horizontal row shows all the sizes of the doubly digested fragments (left to right, small to large). "B" and "E" denote BamH1 and EcoR1 digested fragments, respectively. "S" denotes a fragment which is not digested by the second enzyme, i.e., no cutting site present for the second enzyme. The numerical subscript denotes the order for the linear construction of the original strand DNA.

Figure #6

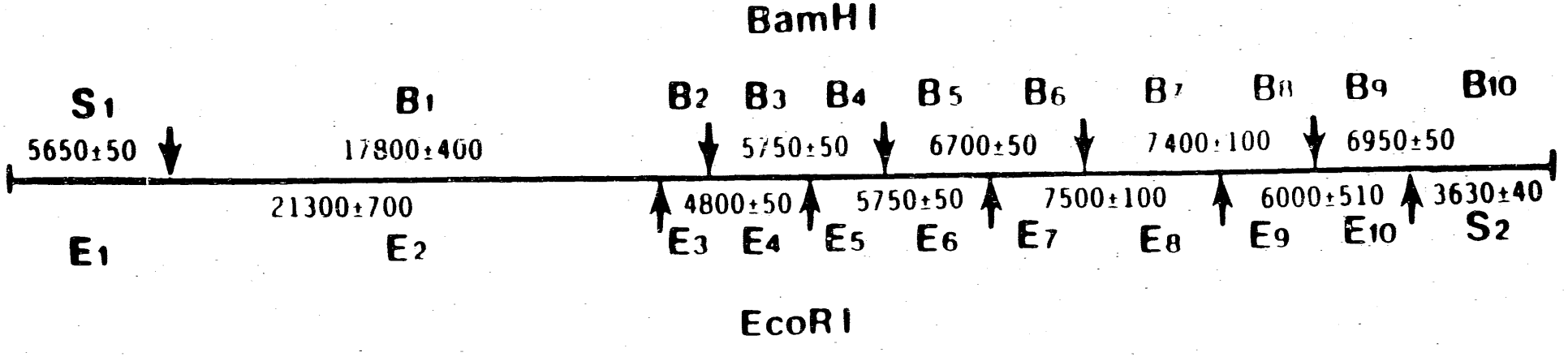

The linear map of lambda phage DNA for the Bam Hl and Eco Rl fragments

Figure #1

a.

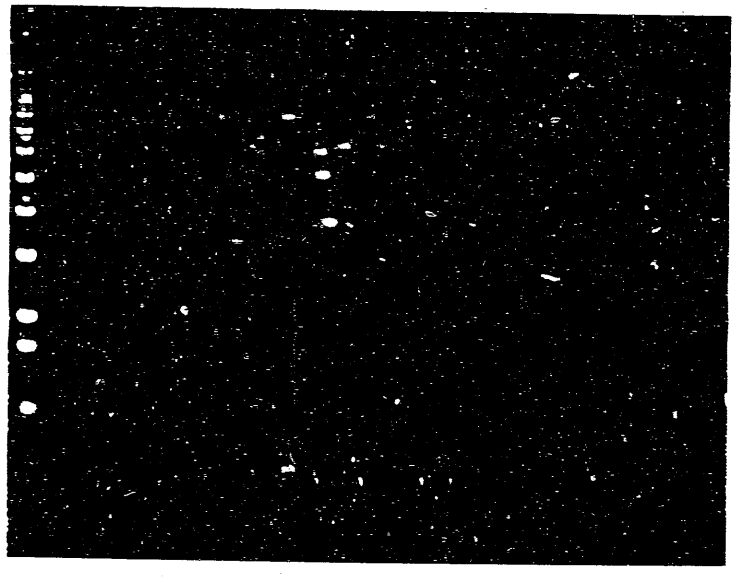

EcoRI → BamHI

b.

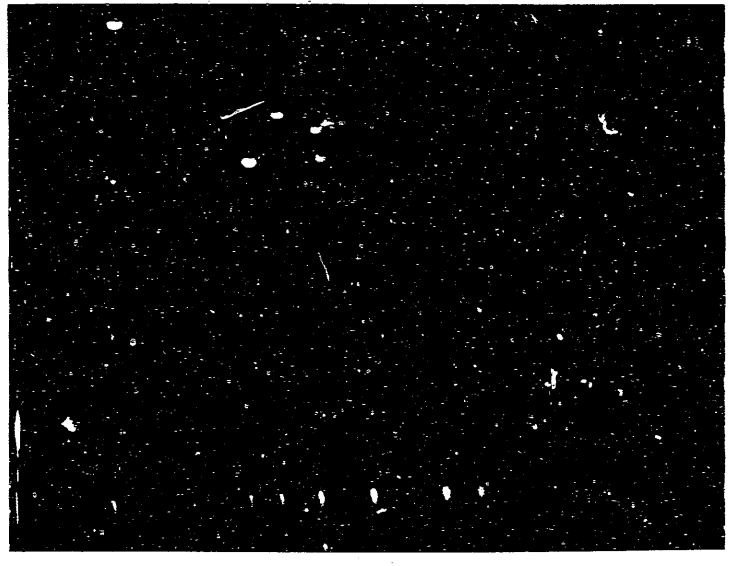

BamHI → EcoRI

c.

M E B EB

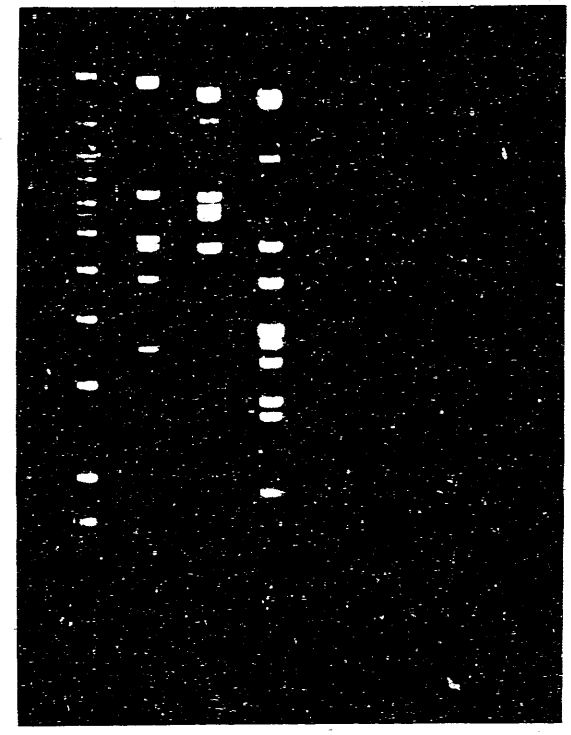

M: marker
E: EcoRI
B: BamHI
EB: EcoRI and BamHI

Figure #8

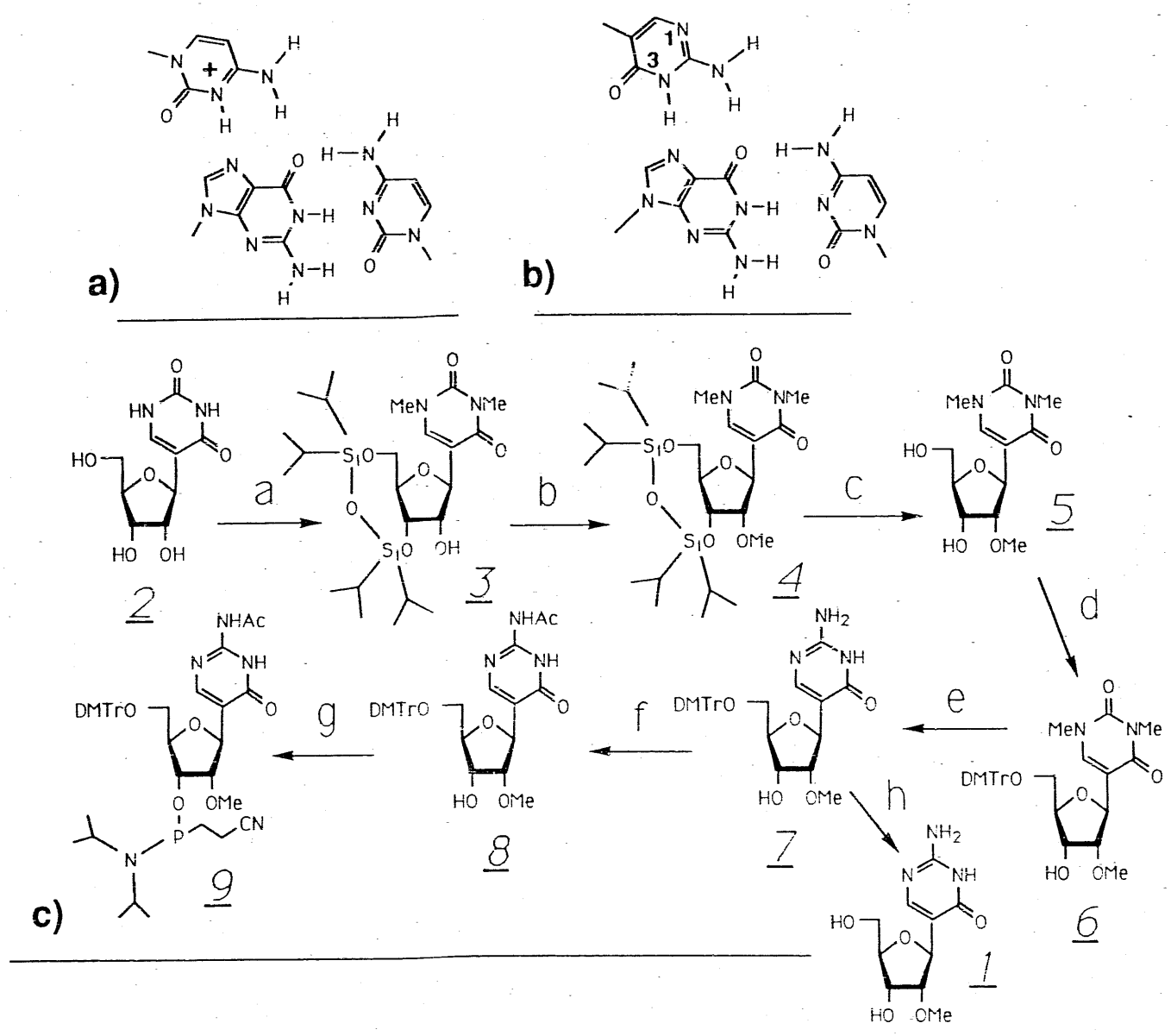

Figure #9

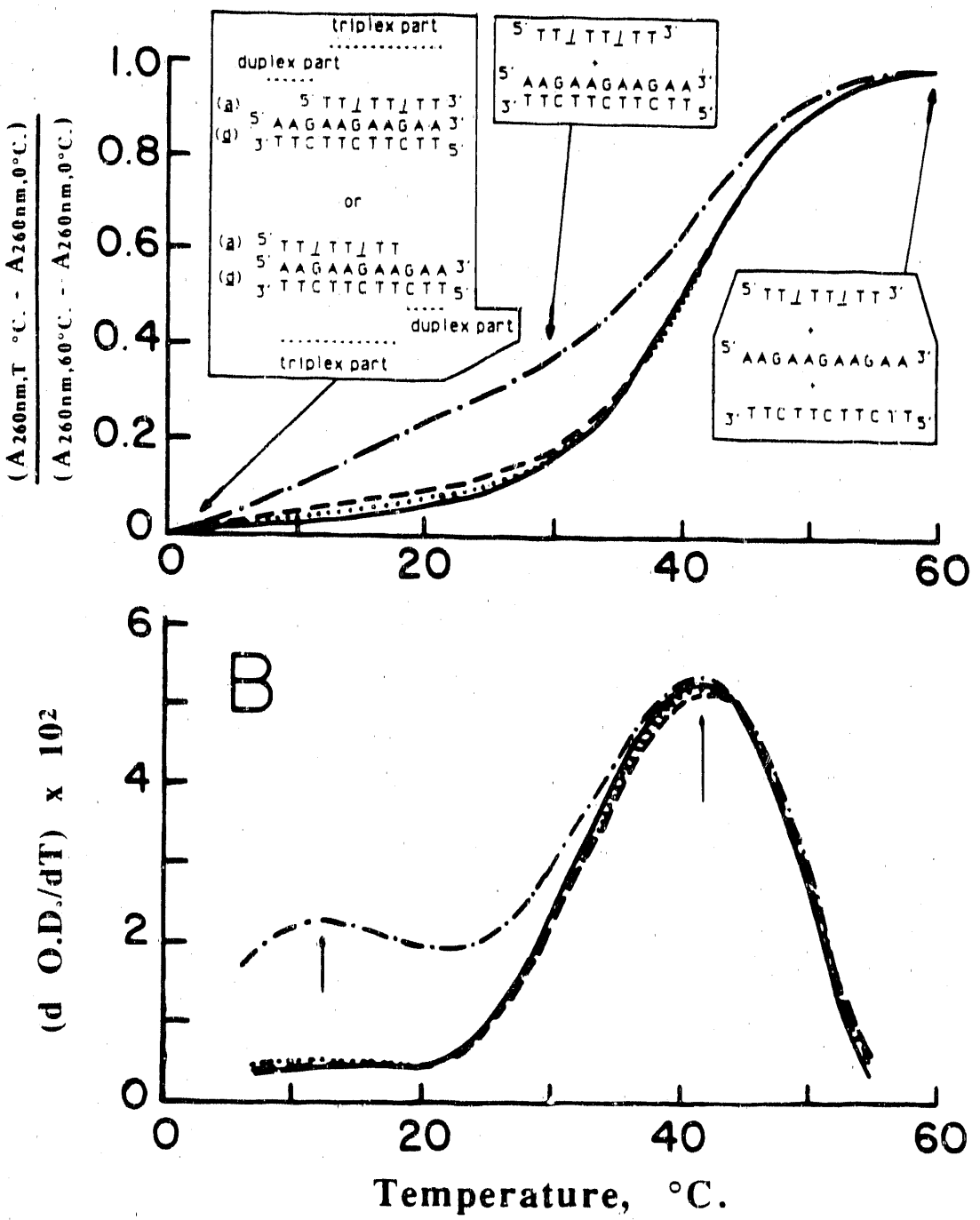
triplex part
duplex part
(a) 5' TTJTTJTT 3'
(g) 5' AAGAAGAAGAA 3'
3' TTCTTCTTCTT 5'
or
(a) 5' TTJTTJTT
(g) 5' AAGAAGAAGAA 3'
3' TTCTTCTTCTT 5'
duplex part
triplex part
5' TTJTTJTT 3'
5' AAGAAGAAGAA 3'
3' TTCTTCTTCTT 5'
5' TTJTTJTT 3'
5' AAGAAGAAGAA 3'
3' TTCTTCTTCTT 5'
(A260nm,T °C. - A260nm,0°C.) / (A260nm,60°C. - A260nm,0°C.)
1.0
0.8
0.6
0.4
0.2
0
0
20
40
60
B
(d O.D./dT) x 10²
6
4
2
0
0
20
40
60
Temperature, °C.

Figure #10

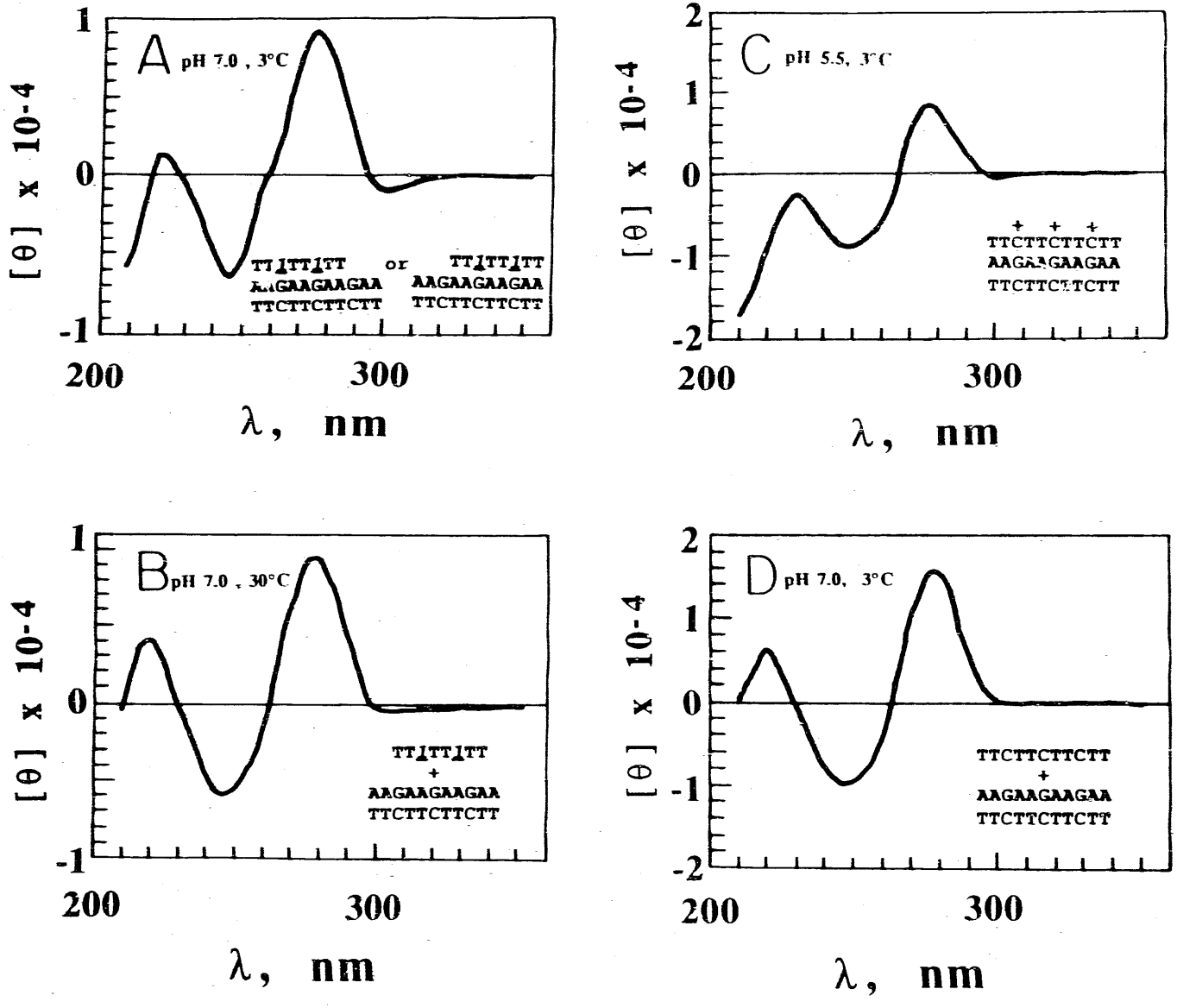
A pH 7.0 , 3°C
TT⊥TT⊥TT or TT⊥TT⊥TT
AAGAAGAAGAA AAGAAGAAGAA
TTCTTCTTCTT TTCTTCTTCTT
C pH 5.5, 3°C
TTCTTCTTCTT
AAGAAGAAGAA
TTCTTCTTCTT
B pH 7.0 , 30°C
TT⊥TT⊥TT
+
AAGAAGAAGAA
TTCTTCTTCTT
D pH 7.0, 3°C
TTCTTCTTCTT
+
AAGAAGAAGAA
TTCTTCTTCTT
[θ] x 10-4
λ, nm
200
300
1
0
-1
2
-2

Table I

DNA Markers Fragments (bp)	Migrated Distances					
	1-D (cm)			2-D (cm)		
	Top	Middle	Bottom	Top	Middle	Bottom
23130	1.40	1.40	1.40	1.30	1.30	1.30
12216	2.45	2.45	2.45	2.25	2.25	2.30
11198	2.65	2.70	2.60	2.45	2.45	2.50
10180	2.95	3.00	3.05	2.75	2.75	2.75
9416	3.20	3.25	3.30	3.00	3.05	3.05
9162	3.30	3.40	3.40	3.10	3.15	3.15
8144	3.75	3.80	3.85	3.50	3.55	3.55
7126	4.30	4.40	4.35	4.00	4.05	4.05
6557	4.55	4.60	4.65	4.25	4.30	4.35
6108	4.95	5.10	5.05	4.65	4.70	4.75
5090	5.85	5.95	5.95	5.45	5.55	5.55
4361	6.55	6.60	6.65	6.15	6.20	6.20
4072	7.00	7.10	7.10	6.55	6.60	6.60
3054	8.50	8.65	8.65	8.00	8.05	8.05
2322	10.75	10.85	10.80	9.45	9.45	9.45
2027 & 2036	11.80	11.95	11.95	10.10	10.10	10.10
1635	14.25	14.30	14.30	11.05	11.10	11.05
1018				13.25	13.25	13.25

The distances (cm) migrated by the individual DNA restriction fragments (λ/Hind III) and size marker fragments (1kb DNA ladder) in the three different layers of gel (top, middle, and bottom) in a two dimensional, three-layer electrophoresis. The biggest difference observed in the mobility of each identical band from the different gel is 0.05 - 0.15cm.

Table II
Melting Temperatures of r-GAUCA Duplexes

Oligomer	T_m °C	
	50 mM Tris	50 nM Tris/ 0.1 M NaCl
d-TGATC	15	22
d-TpGATC	< 9	18
r-$U^mpI^mA^mU^mC$	15	21

List of Appendices *

A. Au, L.-C., Ts'o, P.O.P., Yi, M.: Monitoring Mammalian Genome Rearrangement with Mid-Repetitive Sequences as Probes. Analytical Biochemistry (Accepted).

B. Yi, M., Au, L-C., Ichikawa, N., Ts'o, P.O.P.: Enhanced Resolution of DNA Restriction Fragments: A Procedure by Two-Dimensional Electrophoresis and Double-labeling. Proc. Natl. Acad. Sci., 87(10):3919-3923, 1990.

C. Miller, P.S., Bhan, P., Cushman, C.D., Kean, J.M., Levis, J.T.: Antisense Oligonucleoside Methylphosphonates and Their Derivatives. Nucleosides & Nucleotides (In Press).

D. Kan, L.S.: Proton NMR and Optical Spectroscopic Studies on the DNA Triplex Formed by d-A-(G-A)7-G and d-C-(T-C)7-T. J. Biomolecular Struct. and Dyn., (Accepted).

E. Kan, L.A.: Comparative Circular Dichroism and Fluorescence Studies of Oligodeoxyribonucleotide and Oligodeoxyribonucleoside Methylphosphonate Pyrimidine Strands in Duplex and Triplex Formation. Biochemistry (Accepted).

* removed and cycled reparately —

-END-

DATE FILMED

11 / 1 / 90